International Journal of Constructive Research in Civil Engineering (IJCRCE)
Volume 6, Issue 1, 2020, PP 1-9
ISSN 2454-8693 (Online)
DOI: http://dx.doi.org/10.20431/2454-8693.0601001
www.arcjournals.org

Experimental Study on the High-Temperature Creep Behavior of Super Alloy Using Digital Image Correlation

Yezhuang XU*

Highway Development Center, Department of Transport of Jiangsu Province, Nanjing, China.

Corresponding Author:** ***Yezhuang XU, *Highway Development Center, Department of Transport of Jiangsu Province, Nanjing, China. Email: yzxu901@126.com*

Abstract: *In this work, Digital Image Correlation (DIC)was employed to measure creep strain evolution of superalloy under 1000℃, and grayscale-average technique was proposed to minimize the thermal disturbance and noise effect in high-temperature DIC. First, the principle of grayscale-average technique was introduced, and Zero-mean Normalized Sum of Squared Differences (ZNSSD) criterion was developed to estimate the noise reduction effectiveness of the proposed method. Then experimental verification using computer-simulated speckle images was carried out, and some typical displacement fields were analyzed. Finally, a non-contact high-temperature creep experimental platform was built up, and the creep strain evolution was obtained using grayscale-average technique and DIC method. The results will provide a new tool for charactering the high-temperature creep behavior of super alloy under high-temperature atmosphere environment.*

Keywords: *high-temperature creep; super alloy; digital image correlation; thermal disturbance; grayscale-average technique*

1. INTRODUCTION

High temperature creep behavior is very important for characterizing super alloy, which can provide a better knowledge of the material performance, crack initiation and propagation, and the failure mechanisms that work under extreme conditions. However, it is difficult to employ the contact testing method under extreme conditions. DIC method is widely used to measure deformation and strain for different materials and structures under different loadings and environment conditions, thanks to its advantage of non-contact and full field measurement. Moreover, its experimental setup is simple, requirements of measurement environment is low and the measurement sensitivity and resolution range are wide [1, 2]

Both the measurement principle and the measurement application of high-temperature DIC method have been widely discussed. Pan et al .[3] combined the commonly used iterative spatial-domain cross-correlation algorithm and optical band pass filter imaging scheme and proposed a improved high-performance DIC method for accurate full-field deformation measurements of objects at temperatures up to 1200℃. Dong et al. [4] examined a variety of speckle patterns to identify patterns suitable for micro scale DIC at high temperature up to 1400℃. Dong et al. [5] developed a new high temperature DIC, in which the optical system composed of a UV CCD camera, UV illumination, filter and long-distance lens. Yang et al.[6] developed a high temperature micro digital image correlation method, which include a simple high temperature resistant speckle manufacturing technology, and applied the method to study the real time deformation of thermal barrier coatings' (TBCs) near-interface regions and surfaces during a thermal shock of 1100℃. By combining transient aerodynamic heating simulation device and the reliability-guided digital image correlation (RG-DIC), Pan et al. [7] established a novel non-contact high-temperature deformation measurement system in order to determine the full-field high-temperature thermal deformation of the structural materials used in high-speed aerospace flight vehicles. Meyer and Waas [8] developed a new speckle technique for strain measurements at room and high temperatures up to 1300 °C.

The elementary result from DIC is the displacement fields at a dense grid of points covering the subset of interest. Although the displacement estimates are very accurate, noise is induced in the displacement estimates by several factors such as the choice of interpolation scheme, quality of

speckle pattern, shape function and subset size, optimization scheme and convergence criterion and image distortion due to lens and sensor errors [9-11], especially in high-temperature DIC. The measurement error from the process of image acquisition obtained extensive attention by researchers. Pan et al. [12] studied the systematic errors in two-dimensional digital image correlation due to lens distortion. They proposed a linear least-squares algorithm to estimate the distortion coefficient from the distorted displacement results to eliminate the systematic errors caused by lens distortion. Moreover, they proved that the bilateral telecentric lenses can improve the accuracy of 2D digital image correlation [13]. Also, a generalized compensation method using a non-deformable reference sample was proposed by Pan et al.[14-15]. Recently, the image preprocess method has been used in DIC by the developing of computer technology and high temperature DIC application. Zhou et al.[16] applied a pre-filtering to the images prior to the correlation to suppress the high-frequency contents. Su et al.[17] proposed a grayscale-average technique to improve the measurement accuracy of high-temperature DIC.

In this work, the high-temperature creep behavior of super alloy was investigated using DIC, and the grayscale-average technique was employed to reduce the thermal disturbance and noise in high temperature DIC. Firstly, the experimental verification of grayscale-average technique using computer-simulated speckle images was carried out on several typical deformations. Moreover, a high-temperature creep experiment was conducted on super alloy to evaluate the effectiveness of the proposed method.

2. PRINCIPLE OF GRAYSCALE-AVERAGE TECHNIQUE

2.1. Basic Principle of DIC Method

In the algorithm of DIC method, how to establish corresponding relationship between the image before and after deformation will affect the calculation accuracy. This is a key step of the algorithm. The establishment of corresponding relation is usually based on the following two conditions [18-19]: (1) the image gray level of the same point on the surface before and after deformation stays the same; (2) any image contains enough of the subset and random distributed speckle is uniqueness in the gray level.

In order to realize the request of condition (1) as much as possible, usually a stable and uniform illumination is needed in the actual measurement. In DIC method, the ‘subset’ referred in the conditions (2), is commonly referred to as related areas or related computing area. It is usually an *M*×*M* square area, and the size of the area has certain influence on measurement accuracy. If the area is too small, the amount of information it contains is not enough, and it is difficult to accurately match the related area in speckle image. A big area can cause serious averaged effects; it is also difficult to accurately match the related area in speckle image. In both cases, it will reduce the accuracy of measurement.

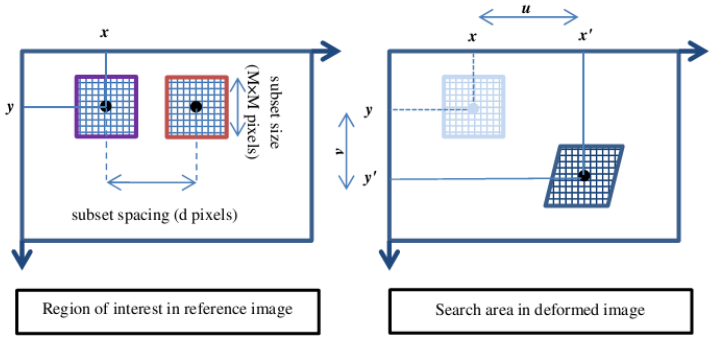

Fig1. *Principle of digital image correlation method*

As shown in Fig.1, the current algorithms for a variety of DIC method, are mostly based on displacement parameters, and establish the mapping relationship between the pixel point on the image before and after deformation. The displacement of the pixel, *(x, y)*, in the image before deformation, is *(u, v)*, which corresponding to the point (x', y') in the image after deformation.

$$\begin{cases} x' = x + u \\ y' = y + v \end{cases} \quad (1)$$

After establishing a mapping relationship, then a relevant formula is selected to calculate the correlation coefficient of image subinterval before and after deformation. Subinterval match is considered the best when the correlation coefficient reaches extreme value. Then displacement can be obtained. At present, the related calculation methods are classified into the following several main ways [20]: (1) double parameters method; (2) the size search method; (3)Newton-Raphson method; (4) cross search method; (5) mountain climbing search method; (6) correlation coefficient gradient method, (7) genetic algorithm; and (8) the fractal algorithm.

2.2. Principle of Grayscale-Average Technique

In order to eliminate the effects of thermal disturbance on the deformation measurement in high-temperature DIC, the grayscale-average technique was developed in this investigation. If N images affected by thermal disturbance at the given temperature are obtained, the grayscale intensity of the affected high-temperature image i at coordinate *(x, y)* can be expressed as [17]

$$g_i(x,y) = f(x,y) + r_i(x,y) \quad (i = 1,2,\cdots,N) \tag{2}$$

Where $r_i(x, y)$ is the grayscale error values caused by the thermal disturbance. For the image i (n×m pixels), the signal to noise ratio (SNR) can be expressed as

$$SNR = \frac{\sum_{x=1}^{n}\sum_{y=1}^{m}\left[f^2(x,y)\right]}{\sum_{x=1}^{n}\sum_{y=1}^{m}\left[g_i(x,y) - f(x,y)\right]^2} = \frac{\sum_{x=1}^{n}\sum_{y=1}^{m}\left[f^2(x,y)\right]}{\sum_{x=1}^{n}\sum_{y=1}^{m}\left[r_i^2(x,y)\right]} \tag{3}$$

After processing N images using the grayscale-average technique, the grayscale intensity at coordinate *(x, y)* can be expressed as

$$\overline{g}(x,y) = \frac{1}{N}\sum_{i=1}^{N} g_i(x,y) = \frac{1}{N}\sum_{i=1}^{N}\left[f(x,y) + r_i(x,y)\right] = f(x,y) + \frac{1}{N}\sum_{i=1}^{N}\left[r_i(x,y)\right] \tag{4}$$

Then the SNR of the images processed by grayscale-average technique can be determined

$$\overline{SNR} = \frac{\sum_{x=1}^{n}\sum_{y=1}^{m}\left[f^2(x,y)\right]}{\sum_{x=1}^{n}\sum_{y=1}^{m}\left[\overline{g}(x,y) - f(x,y)\right]^2} = \frac{\sum_{x=1}^{n}\sum_{y=1}^{m}\left[f^2(x,y)\right]}{\sum_{x=1}^{n}\sum_{y=1}^{m}\left[\frac{1}{M}\sum_{i=1}^{N} r(x,y)_i\right]^2} \tag{5}$$

Thus, it can be derived from Eqs. (3) and (5) that

$$\overline{SNR} = N^2 SNR \tag{6}$$

It is evident that the SNR of the processed images using the grayscale-average technique in DIC calculation is N2 times compared to the SNR of the unprocessed single image, which accounts for great improvement in grayscale quality of high-temperature images.

2.3. Experimental Verification using Computer-Simulated Speckle Images

In order to verify the practicability of grayscale-average technique, the simulated speckle images are implemented by means of image correlation for displacement calculation. For the simulated speckle images, three different conditions are considered as: (1) the original speckle images; (2) the speckle images with disturbance; (3) the speckle images with disturbance processed by grayscale-average technique (N=25)[17]. Uniform translation represents the simplest homogeneous deformation that can be studied and is chosen to validate the results of the proposed technique against ground truth. The simulated speckle images at 1000℃were synthesized according to [17], which is shown in Fig. 2. In this investigation, the characteristic parameters of the simulated speckle images are designed as follows: The size of image is 500×500 pixels; the characteristic length of speckle particle is three pixels; the number of speckle particle is 3500. To simulate uniform translation under high-temperature environment, the typical uniform translation configurations are used to generate the speckle image pairs before and after translation as follows:

$$X_k' = X_k + U_0 \tag{7}$$

$$Y_k' = Y_k + V_0 \tag{8}$$

Where U0 and V0are the preset displacement components. In this study, these preset values are: U0=15 pixels, V0=15 pixels.

DIC is performed on the reference and deformed images using an in-house code employing Newton-Raphson algorithm. 25×25 pixel subsets with an overlap of 20 pixels between successive subsets are used in computing the displacement fields, resulting in 54×54 U and V matrices. In order to analyze the effect of noise, simulated speckle images with SNR values of 50 dB and 100 dB are also generated.

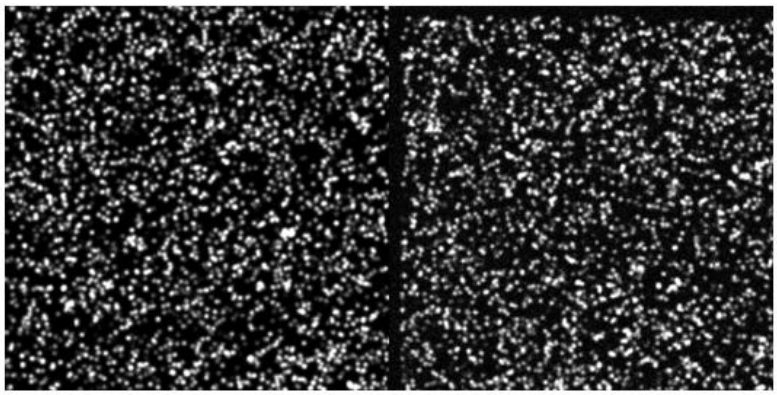

(a) Referenced speckle image (without noise) (b) Deformed speckle image at 1000 ℃ (SNR=50dB)

Fig2. *Simulated speckle images (500×500 pixels)*

The displacement errors of the images without noise, which are difference between the displacement field from DIC and preset uniform translation (U0 and V0), are shown in Fig. 3. It is evident that the displacement calculated from the speckle image without thermal disturbance is almost equal to the pre-set value. However, the displacement errors from the images with thermal disturbance are about 0.5 pixels. Moreover, the displacement errors calculated from the images after grayscale-average by 25 images are about 0.2 pixels, which are less than half of the displacement errors before grayscale-average. Therefore, the displacement errors are reduced by the process of the grayscale-average technique substantially.

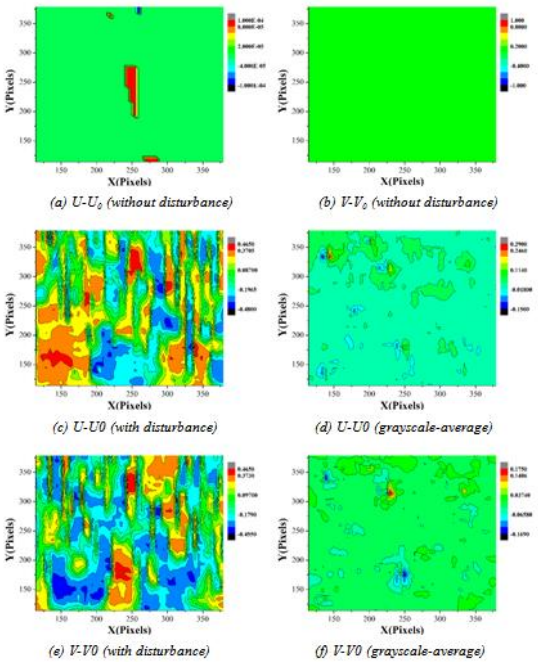

Fig3. *Displacement error from DIC (noise free, unit: pixels)*

In addition, Fig. 4 shows the pseudo strain from DIC without noise, which are calculated from the displacement fields in Fig. 3. Although the simulated images only contain uniform translation, there are 22800με normal strain on x-direction, 9700με normal strain on y-direction and 9700με shear strain, which are pseudo strain caused by the thermal disturbance and noise.It is evident that the pseudostrain calculated from the images after grayscale-average are at least one order of magnitude smaller.In light of these observations, it is clear that the proposed method has effectiveness on the pseudo strain reduction caused by thermal disturbance.

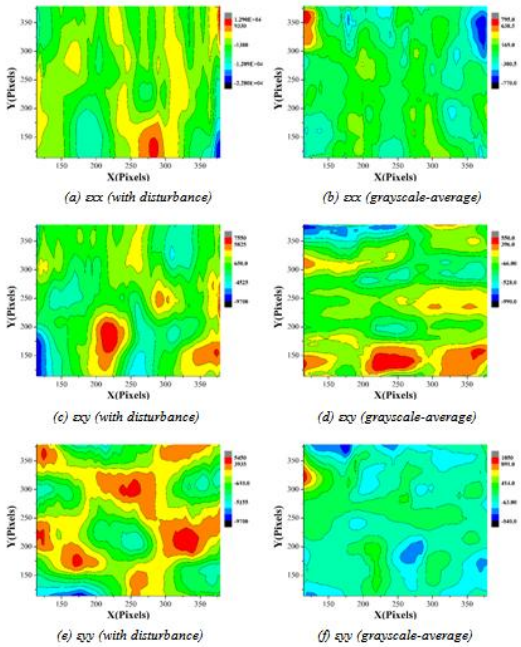

Fig4. *Pseudo strain from DIC (noise free, unit: με)*

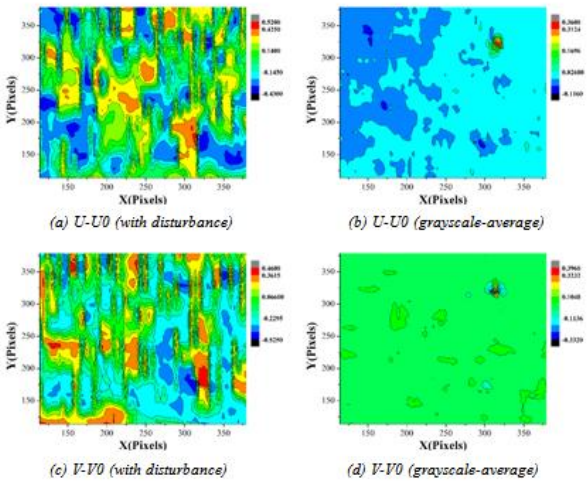

Fig5. *Displacement error from DIC (SNR=100dB, unit: pixels)*

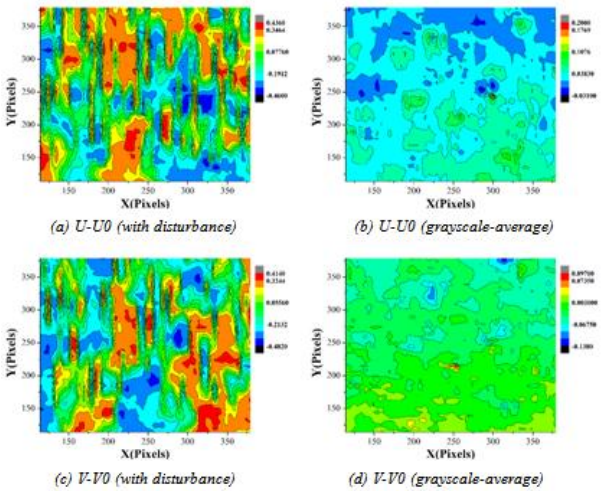

Fig6. *Displacement error from DIC (SNR=50dB, unit: pixels)*

In order to investigate the effectiveness of grayscale-average technique on the images contain different levels of noise, images with SNR values of 50 dB and 100 dB are generated using computer-

simulated speckles. The displacement errors between the displacement fields, calculated from the images with SNR values of 50 dB and 100 dB, and the present value are shown in Fig. 5 and Fig. 6, respectively. Moreover, the corresponding pseudo strain caused by the thermal disturbance and noise are shown in Fig. 7 and Fig. 8, respectively. It is also worth noting that the displacement errors calculated from the processed images by grayscale-average are smaller than that before processed in both cases. It is worth highlighting that the pseudo strain caused by the non-uniform displacement errors are also decreased by one order of magnitude after processed by grayscale-average. The value of pseudo strain with thermal disturbance is on the level of 10000με, yet they decrease to less than 1000μεafter processed by grayscale-average. Therefore, a similar variation characteristic as that obtained by the proposed method can be also observed.

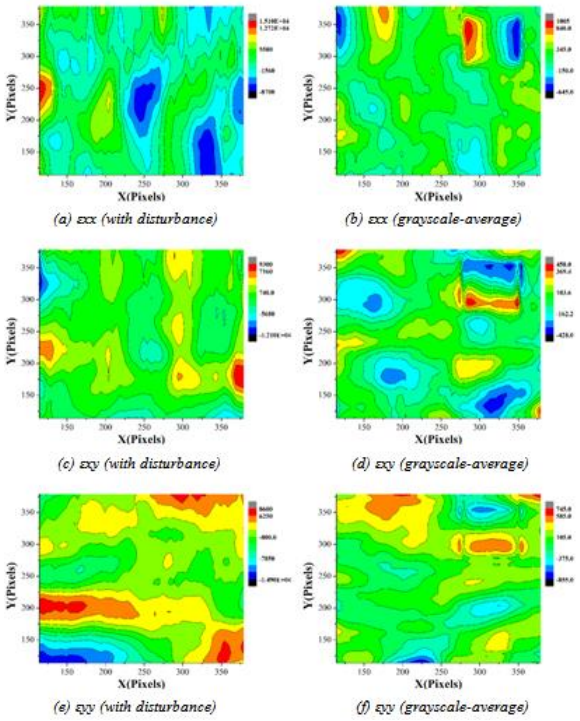

Fig7. *Pseudo strain from DIC (SNR=100dB, unit: με)*

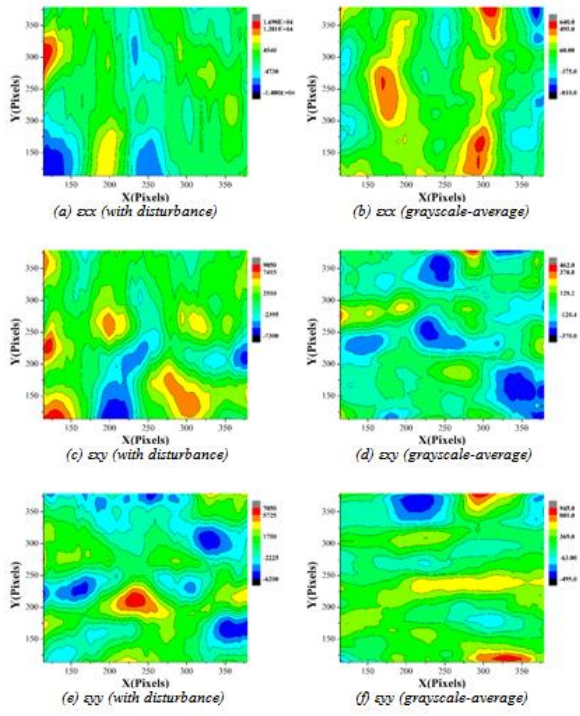

Fig8. *Pseudo strain from DIC (SNR=50dB, unit: με)*

3. HIGH-TEMPERATURE CREEP EXPERIMENT

3.1. Specimen Preparation

In this investigation, a nickel-base single crystal super alloy (DD6) sample of 20mm×3mm×1 mm was used as a reference specimen. DD6 has been widely used in aerospace engineering as a structural material thanks to its excellent performance of plasticity, ductility and extrusion. Commercially available zirconium oxides paint were applied to the super alloy surface by an air-brush with a nozzle size of 0.8 mm, at a distance of 500-600mmawayfromthesamplesurface. The paint was composed of 75% powder and 25% binder by weight. The zirconium oxides paint was air dried at room temperature for 1 hour, cured at 93℃for2 hours, and finally cured at 260℃ for 1-2 hours before being heated at high temperature. The specimen with speckles under 1000℃ is shown in Fig. 9.

Fig9. *Specimen with speckles under 1000 ℃*

3.2. Experimental Setup

The DIC experimental set up for high-temperature creep is shown in Fig. 10, which consists of a heating furnace with an optical observation window (quartz glass) and a temperature control box. The optical observation window was fastened on the heating furnace by a metal frame and several screws, which was surrounded by the refractory materials made from quartz. Here, the thermal radiation was suppressed by means of optical band pass filter (central wavelength 473 nm). A CCD camera was employed to capture the images, and the light source was used to supply sufficient light. The specimen was heated using the electric resistance furnace to 1000℃ at a rate of 50℃/min

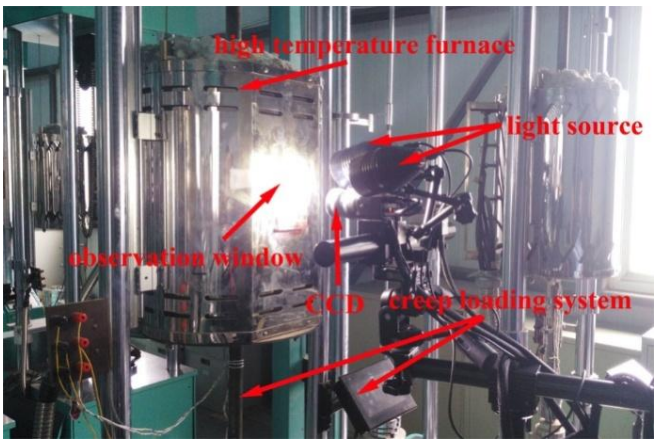

Fig10. *Experimental set up for high-temperature creep*

3.3. Results and Discussion

To verify the practicality of the proposed method for reducing pseudo strain caused by thermal disturbance and noise, a tensile creep experiment was conducted on super alloy under high-temperature up to 1000℃ using DIC and grayscale-average technique.

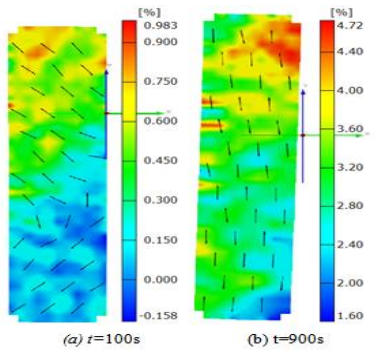

Fig11. *Full-field strain distribution*

Fig. 11 shows the full-field strain calculated using DIC, where Fig. 11(a) is the normal strain distribution along the length direction of the specimen at t=100s and Fig. 11(b) is the normal strain distribution along the length direction of the specimen at t=900s. It is evident that the direction of normal strain is not absolutely along the loading direction, which is caused by the thermal disturbance in the capture images. However, the effect of thermal disturbance is reduced with the increasing of creep strain, and the strain distribution is tending to uniform(Fig. 11(b)). Therefore, the effect of thermal disturbance on the high-temperature creep strain is substantially obvious.

The strain between two points in the middle of the specimen was taken from the full-field strain as the research object. The creep strain evolution with time is shown in Fig. 12. The strain in Fig. 12(a) was calculated from the single image capture by the CCD, as well as the strain in Fig. 12(b) was calculated from the image processed by grayscale-average technique using 25 images. It is obvious that the strain evolution curve in Fig. 12(b) is smoother than that in Fig. 12(a), which means that the effect of thermal disturbance is reduced after processed by grayscale-average technique. Therefore, a similar variation characteristic as that obtained by simulated speckles can be also observed by the high-temperature creep experiment.

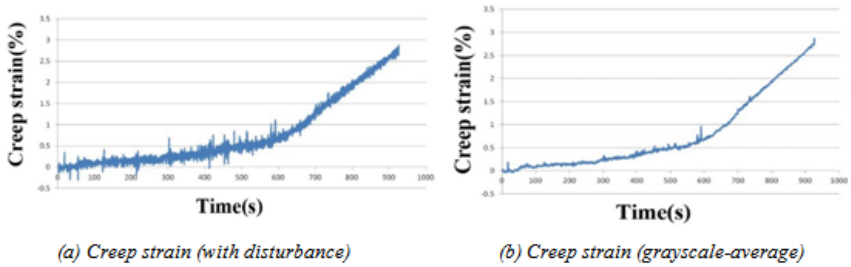

Fig12. *Creep strain evolution curves*

4. CONCLUSION

In this work, the high-temperature creep behavior of super alloy was investigated using DIC method and grayscale-average technique. Some important conclusions are summarized as follow:

- The principle of grayscale-average technique was developed, and experimental verification of the proposed method was conducted using computer-simulated speckle images. The results show that the displacement errors caused by thermal disturbance and noise can be reduced by grayscale-average technique substantially. The pseudo strain calculated from the grayscale-averaged images is at least one order of magnitude smaller than that before processed.
- The effectiveness of grayscale-average technique on the noise speckle images was investigated using computer-simulated speckle images with SNR values of 50 dB and 100 dB. The simulated results show a similar variation characteristic as that obtained in the noise-free case by the proposed method.
- To verify the practicality of the proposed method for reducing pseudo strain caused by thermal disturbance and noise, a tensile creep experiment was conducted on super alloy under high-temperature up to 1000℃ using DIC and grayscale-average technique. Commercially available zirconium oxides paint were applied to the super alloy surface by an air-brush with a nozzle size of 0.8 mm, at a distance of 500-600mm away from the sample surface to act as speckles. The

creep strain evolution curves were obtained using DIC, which are calculated from the images before and after processed by grayscale-averaged images.

REFERENCES

[1] B. Pan, K. Qian, H.Xie, A. Asundi. Two-dimensional digital image correlation for in-plane displacement and strain measurement: a review. Meas Sci Technol (2009), 62001.

[2] W. Hao, D. Ge, Y. Ma, X. Yao, Y. Shi. Experimental investigation on deformation and strength of carbon/epoxy laminated curved beams. Polym Test. 31 (2012), 520-526.

[3] B. Pan, D. Wu, Z. Wang, Y. Xia. High-temperature digital image correlation method for full-field deformation measurement at 1200 °C. Measurement Science and Technology. 22 (2011), 15701.

[4] Y. Dong, H. Kakisawa, Y. Kagawa. Development of microscale pattern for digital image correlation up to 1400°C. Opt Laser Eng. 68 (2015), 7-15.

[5] Y. Dong, H. Kakisawa, Y. Kagawa. Optical system for microscopic observation and strain measurement at high temperature. Measurement Science and Technology. 25 (2014), 25002.

[6] X. Yang, Z. Liu, H. Xie. A real time deformation evaluation method for surface and interface of thermal barrier coatings during 1100 °C thermal shock. Measurement Science and Technology. 23 (2012), 105604.

[7] B. Pan, D. Wu, Y. Xia. High-temperature deformation field measurement by combining transient aerodynamic heating simulation system and reliability-guided digital image correlation. Opt Laser Eng. 48 (2010), 841-848.

[8] P. Meyer, A.M. Waas. Measurement of In Situ-Full-Field Strain Maps on Ceramic Matrix Composites at Elevated Temperature Using Digital Image Correlation. Exp Mech. 55 (2015), 795-802.

[9] M.Y. Dehnavi, S. Khaleghian, A. Emami, M. Tehrani, N. Soltani. Utilizing digital image correlation to determine stress intensity factors. Polym Test. 37 (2014), 28-35.

[10] I. Eshraghi, M.R. Yadegari Dehnavi, N. Soltani. Effect of subset parameters selection on the estimation of mode-I stress intensity factor in a cracked PMMA specimen using digital image correlation. Polym Test. 37 (2014), 193-200.

[11] M.R. Yadegari Dehnavi, I. Eshraghi, N. Soltani. Investigation of fracture parameters of edge V-notches in a polymer material using digital image correlation. Polym Test. 32 (2013), 778-784.

[12] B. Pan, L. Yu, D. Wu, L. Tang. Systematic errors in two-dimensional digital image correlation due to lens distortion. Opt Laser Eng. 51 (2013), 140-147.

[13] B. Pan, L. Yu, D. Wu. High-accuracy 2D digital image correlation measurements with bilateral telecentric lenses: error analysis and experimental verification. Exp Mech. 53 (2013), 1719-1733.

[14] B. Pan, L. Yu, D. Wu. High-accuracy 2D digital image correlation measurements with low-cost lenses: implementation of a generalized compensation method. Meas Sci Technol. 25 (2014), 25001.

[15] L. Yu, B. Pan. In-plane displacement and strain measurements using a camera phone and digital image correlation. Opt Eng. 53 (2014), 54107.

[16] Y. Zhou, C. Sun, Y. Song, J. Chen. Image pre-filtering for measurement error reduction in digital image correlation. Opt Laser Eng. 65 (2015), 46-56.

[17] Y.Q. Su, X.F. Yao, S. Wang, Y.J. Ma. Improvement on measurement accuracy of high-temperature DIC by grayscale-average technique. Opt Laser Eng. 75 (2015), 10-16.

[18] B. Pan, H. Xie, Z. Guo, T. Hua. Full-field strain measurement using two-dimensional Savitzky-Golay digital differentiator in digital image correlation. Opt Eng 46(2007), 33601.

[19] J. Abanto-Bueno, J. Lambros. Investigation of crack growth in functionally graded materials using digital image correlation. Eng Fract Mech. 69 (2002), 1695-1711.

[20] B. Pan, Z. Wang. Recent progress in digital image correlation. In: T. Proulx. (Ed.). Application of Imaging Techniques to Mechanics of Materials and Structures, Volume 4. Springer New York2013. pp. 317-326.

Citation: *Yezhuang XU, "Experimental Study on the High-Temperature Creep Behavior of Super Alloy Using Digital Image Correlation", International Journal of Constructive Research in Civil Engineering, 6(1), pp. 1-9. DOI: http://dx.doi.org/10.20431/2454-8693.0601001.*